

See discussions, stats, and author profiles for this publication at: <https://www.researchgate.net/publication/231633076>

High-Resolution Spectroscopic Study of Matrix-Isolated Reactive Intermediates: Vibrational Assignments for 3-Fluoro-o-Benzyne and Perfluoro-o-Benzyne ∇

ARTICLE in THE JOURNAL OF PHYSICAL CHEMISTRY A · JUNE 2002

Impact Factor: 2.69 · DOI: 10.1021/jp0209998

CITATIONS

8

READS

19

4 AUTHORS, INCLUDING:



J. Waluk

Polish Academy of Sciences

254 PUBLICATIONS 3,665 CITATIONS

SEE PROFILE



Jens Spanget-Larsen

Roskilde University

192 PUBLICATIONS 1,666 CITATIONS

SEE PROFILE

High-Resolution Spectroscopic Study of Matrix-Isolated Reactive Intermediates: Vibrational Assignments for 3-Fluoro-*o*-Benzyne and Perfluoro-*o*-Benzyne[▽]

J. George Radziszewski,^{*,†,‡,§} Jacek Waluk,^{†,‡,§} Piotr Kaszynski,[⊥] and Jens Spanget-Larsen^{†,‡,||}

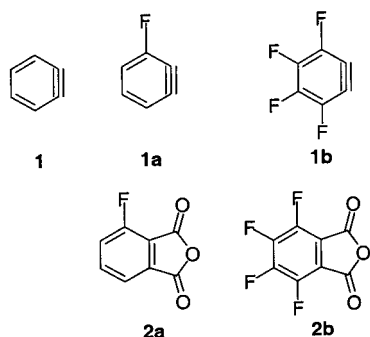
National Renewable Energy Laboratory (NREL), 1617 Cole Blvd. Golden, Colorado 80401, Department of Chemical Engineering, Colorado School of Mines, Golden, Colorado 80401, ADA Technologies, Inc., Littleton, Colorado 80127, Institute of Physical Chemistry, Polish Academy of Sciences, Kasprzaka 44, 01-224 Warsaw, Poland, Department of Chemistry, Vanderbilt University, Nashville, Tennessee 37235, and Department of Chemistry, Roskilde University (RUC), DK-4000 Roskilde, Denmark

Received: April 18, 2002

A novel “site decompression technique” that takes advantage of specific pressure relaxation effects in cryogenic noble gas matrices was applied in a spectroscopic investigation of the two title compounds, resulting in virtually background-free, complete, high-resolution IR spectra with line widths of ca. 0.1 cm⁻¹. The compounds were prepared photochemically in Ar and Ne matrices and, together with the related intermediates, fluorinated benzocyclopropenone and cyclopentadienylideneketene, characterized by IR and UV–visible absorption spectroscopy. Weak IR absorption bands observed at 1878 cm⁻¹ for perfluoro-*o*-benzyne and at 1866 cm⁻¹ for 3-fluoro-*o*-benzyne were assigned to CC triple bond stretching vibrations, corresponding to the transition at 1846 cm⁻¹ in the parent *o*-benzyne. The application of polarization spectroscopy on photooriented samples led to the determination of transition moment directions for most of the observed vibrational transitions. Absolute IR absorption intensities were also obtained. The assignments of the observed transitions were supported by the results of B3LYP/cc-pVDZ quantum chemical calculations.

1. Introduction

Arynes containing a highly reactive formal triple bond continue to attract attention of theoreticians as well as experimentalists.^{1–38} One of the most scrutinized reactive intermediates in this class is *o*-benzyne (**1**), extensively utilized



in organic synthesis and mechanistic studies.^{1–3} Despite a long history of efforts directed toward understanding its properties, basic spectroscopic characterization was provided only recently.^{6,15,16,23,24} The vibrational spectrum is still not completely established and continues to be a subject of discussion.³⁷ In an attempt to clarify and reinforce earlier spectral assignments for **1**, we have prepared 3-fluoro-*o*-benzyne (**1a**) and perfluoro-*o*-benzyne (**1b**) by photolysis of the corresponding phthalic

anhydrides (**2a** and **2b**). During the preparation of this manuscript, we became aware of the recent spectroscopic studies by Wenk and Sanders,³⁸ which also included **1b**.

Our initial intent for the IR studies was to enhance the intensity of the triple bond stretching fundamental in **1a** by the presence of a single fluorine atom in a “highly asymmetrical” position. This would help in a definitive assignment of this vibration, which has been the subject of some controversy.³⁶ Preliminary results of ab initio calculations (HF/6-31G*) performed for **1a** indeed suggested that the intensity of this band should be much higher than that in **1**. Higher-level calculations tend to predict a smaller vibrational intensity for the triple bond stretch in **1a**, albeit still significantly larger than in the case of **1** and **1b**. Our experimental observations concur with this finding.

The photochemical investigation of fluorobenzyne was also motivated by our previous discovery of an interesting photochemical ring-opening path for parent *o*-benzyne.⁶ Excitation of matrix-isolated *o*-benzyne with 248 or 193 nm light leads to nearly quantitative formation of hex-1-ene-3,5-diyne. In view of the very small number of reported fluorinated acetylenic compounds, this photochemical path should be of interest as a potential way of preparing such derivatives. Also, the exceptional chemistry of perfluoro-*o*-benzyne (**1b**) warrants further studies of this reactive intermediate. While the reactivity of 3-fluoro-*o*-benzyne (**1a**) is similar to that of parent benzyne (**1**), perfluoro-*o*-benzyne (**1b**) is characterized by a much higher electrophilicity and reactivity than that of the parent compound.³⁹ This is manifested, for instance, in the Diels–Alder reaction of **1b** with thiophene in which the parent *o*-benzyne is unreactive.⁴⁰ Benzyne **1b** also reacts with benzene and its derivatives, giving 1,4-adducts in much higher yield than other halobenzyne and benzyne itself.⁴¹ Another example of the high reactivity of **1b**

[▽] Dedicated to Dr. Petr Čásky on the occasion of his 60th birthday.

^{*} To whom correspondence should be addressed.

[†] National Renewable Energy Laboratory (NREL).

[‡] Colorado School of Mines.

[§] ADA Technologies, Inc..

[#] Polish Academy of Sciences.

[⊥] Vanderbilt University.

^{||} Roskilde University (RUC).

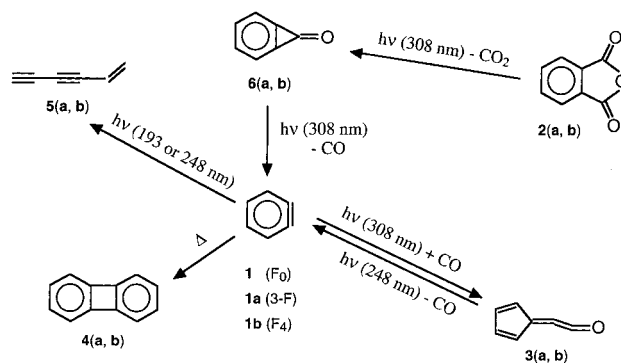
is observed in the reaction with 9-alkylanthracene. While in case of benzyne and other halobenzyne, this reaction leads to 1,4-addition at the anthracene 9,10-positions, yielding triptycenes as sole products, **1b** forms 1,4-adducts with the central and the peripheral anthracene rings in a 3:2 ratio.⁴² The high electrophilicity of **1b** is also apparent from its reactions with ethers, sulfides, and amines.⁴³ The 3-fluoro-*o*-benzyne, **1a**, has been less scrutinized than perfluoro-*o*-benzyne, **1b**, but it has been quite frequently used in mechanistic studies of regioselectivity of nucleophile addition,⁵ as well as in the synthesis of specifically fluorinated compounds.⁴⁴

2. Experimental and Computational Details

The fluorinated *o*-benzyne **1a** and **1b** were prepared by photolysis of the corresponding phthalic anhydrides (**2a** and **2b**) isolated in cryogenic matrices, according to procedures previously discussed in detail.^{6,17} Thus, the fluorinated phthalic anhydride (**2**) was sublimed at 26–32 °C into a stream of noble gas (1–3 mmol/min) and condensed on a cold CsI target. The matrix isolation ratio was always lower than 1:500. The estimates of the precursor (**2a** or **2b**) concentration (and matrix ratio) were made by combining the measurement of the matrix thickness⁴⁵ and the knowledge of the extinction coefficient obtained from the solution. Although there is a change in the bandwidth of the vibronic components of the absorption of **2a** or **2b**, and therefore in the extinction coefficients between room temperature solution and the matrix, the lower limit of the matrix ratio (concentration) can be readily determined. The temperature of the spectroscopic window during the matrix deposition was maintained at 28 K for Ar and 4.2 K for Ne. The Ar matrices were annealed 2–3 times by cycling temperature between 7 and 32 K. The deposition temperature of 28 K for argon matrices is routinely used in our laboratory (and by others) to prepare good optical quality samples required for photochemical transformations and polarization studies. With the rare exceptions of highly polar compounds, the aggregation in this concentration regime is negligible and does not seem to lead to noticeable amounts of additional photoproducts. The diffusion of molecules with a size comparable to the anhydride **2** is still fairly slow at 28 K, and the aggregation level is mostly determined just by the initial concentration in the gas phase. Use of lower deposition temperatures can eliminate diffusion, but it tends to produce frosty samples that preclude penetration of light without unwanted scattering. The anhydride was subsequently photolyzed, and the infrared spectra were recorded by using a FTIR spectrophotometer (Nicolet Magna 560) with 0.125 cm⁻¹ resolution. During the spectroscopic measurements and laser irradiations, the Ar matrices were kept at temperatures around 7 K; for Ne, a temperature of 4.2 K was necessary at all times. The low temperatures were maintained by the use of closed cycle refrigerators, either a two-stage Displex (6.5 K) or a three stage Heliplex (4.2 K) unit (APD Cryogenics). An excimer laser (Lambda Physik) was used to induce the photochemical transformations, generating monochromatic radiation at 193 nm (ArF), 248 nm (KrF), 308 nm (XeCl), and 351 nm (XeF). In some experiments, the 356 nm light from an Ar-ion laser (Coherent I-200) was used or the tunable, doubled output from a ring dye laser.

FTIR polarization spectra were recorded by using a Nicolet FTIR (Magna 850) instrument and a Cambridge Physical Sciences polarizer (IPG-225). The resolution was 0.5 cm⁻¹. Far-infrared peaks were measured on a Nicolet F-20 vacuum bench. UV–visible polarization spectra were measured on a Shimadzu 3100 spectrophotometer equipped with Glan–Thompson polarizers.

SCHEME 1: Photochemical and Thermal Transformations of Fluorinated Anhydrides and *o*-Benzyne



The anhydrides **2a** and **2b** were obtained by dehydration of the corresponding fluorinated phthalic acids with acetic anhydride, according to standard procedures. The 3-fluoro- and perfluorophthalic acids were purchased from Lancaster Synthesis (99% purity).

For geometry optimization and calculations of vibrational frequencies, ab initio HF/6-31G*, MP2/6-311G**, and DFT B3LYP/cc-pVDZ quantum chemical calculations were performed according to standard procedures implemented in the Gaussian 98 suite of programs.⁴⁶

3. Results and Discussion

Irradiation of the matrix-isolated anhydrides **2** with the 308 nm light produces CO₂ and cyclopropanones (**6**). Absorption of subsequent 308 nm photons converts **6** into a mixture of *o*-benzyne (**1**), CO, and cyclopentadienylideneketenes (**3**). Continued irradiation of the sample at 248 nm rapidly transforms ketenes **3** back into *o*-benzyne **1**, while the latter are slowly transformed into diynes, **5** (somewhat faster at 193 nm). Warm-up of the samples containing *o*-benzyne leads to the formation of the biphenylenes, **4**, which can be identified by GC–MS, and provides direct chemical evidence for structure **1**. Scheme 1 indicates the path of the anhydride photolysis and some of the photoinduced and thermal reactions of the resulting *o*-benzyne.

Using such procedures and taking advantage of the site decompression technique described below, we have obtained exceedingly clean and resolved infrared absorption spectra of 3-fluoro-*o*-benzyne (**1a**) and perfluoro-*o*-benzyne (**1b**). They are presented in the bottom segments of Figures 1 and 2. These species were prepared by photolysis of the appropriate fluorinated anhydrides at 308 or 248 nm in Ar or Ne matrixes at 4.2–6 K. The top portions of these figures show a graphical representation of the fundamental vibrational transitions predicted within the B3LYP/cc-pVDZ approximation. The general consistency between experimental and theoretical results supports the assignment of the observed vibrational modes. Additionally, the assignment is aided by the polarization spectra (see below), which provide information on the symmetries of the observed vibrational transitions.

The peak positions and absolute intensities for the experimental and theoretical data are listed in Tables 1 and 2. For comparison, we include in Table 3 the previously reported⁶ vibrational transitions for the parent benzyne **1**, together with the presently calculated data. Figure 3 shows the computed molecular equilibrium geometries for **1**, **1a**, and **1b**. The absolute IR intensities for the benzyne were obtained by comparison of the observed peak areas to those observed for CO and CO₂, of which the absolute intensities have been measured indepen-

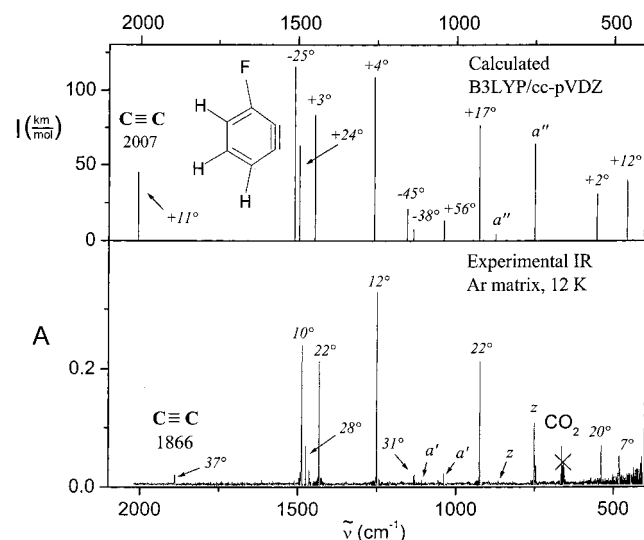


Figure 1. Infrared absorption spectrum of 3-fluoro-*o*-benzyne (**1a**) isolated in an Ar matrix at 12 K (bottom). Theoretical transitions calculated with B3LYP/cc-pVDZ (unscaled) are presented at the top.

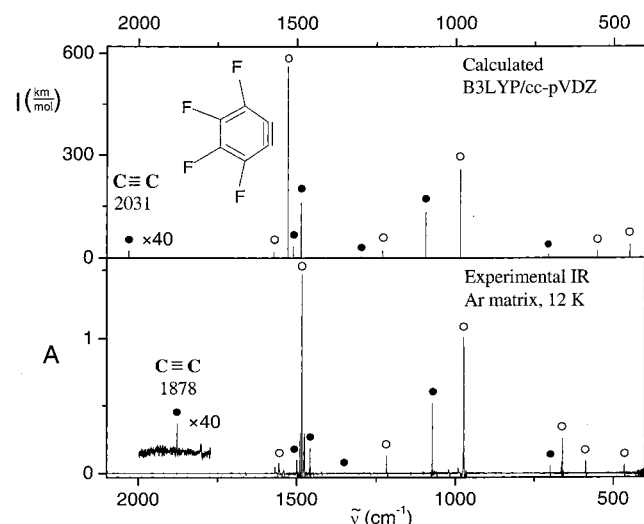


Figure 2. Infrared absorption spectrum of the compressed form of perfluoro-*o*-benzyne (**1b**) isolated in an Ar matrix at 12 K (bottom). Theoretical transitions calculated with B3LYP/cc-pVDZ (unscaled) are presented at the top. Solid dots indicate a_1 vibrations; open circles indicate b_2 vibrations.

dently.⁶ The estimation of the absolute infrared intensities is possible because of the nearly one-to-one stoichiometric ratio of benzyne, CO, and CO₂ under conditions indicated in Scheme 1 and described in the text below. As can be seen from Figures 1 and 2 and from Tables 1 and 2, the agreement between observed and computed relative intensities is very good, particularly for all strong transitions.

The results of this study are consistent with an earlier assignment of the triple bond stretching fundamental for **1**, corresponding to a weak transition observed at 1846 cm⁻¹.⁶ The corresponding transition for 3-fluoro-*o*-benzyne (**1a**) appears at 1866 cm⁻¹, while for perfluoro-*o*-benzyne (**1b**) it is found at 1878 cm⁻¹. As can be seen from Figures 1 and 2, the intensities of the triple bond stretching fundamentals for the fluorobenzyne are still quite low, but the band is significantly stronger for 3-fluoro-*o*-benzyne. The observed frequency shifts, in particular, for the triple bond vibration between **1a** and **1b** are reproduced

TABLE 1: Observed and Calculated Fundamental Vibrational Transitions for 3-fluoro-*o*-benzyne (1a**)^a**

	exptl			B3LYP/cc-pVDZ			approximate description
	$\tilde{\nu}$	I	$ \phi ^b$	$\tilde{\nu}^c$	I	ϕ^b	
$\nu_1 a'$	3108	0.2		3235	2.90	+40	C–H str
ν_2	3077	<0.1		3204	1.46	–43	C–H str
ν_3	3054	0.2		3177	2.86	+33	C–H str
ν_4	1866	3.9	37	2007	45.30	+11	C ₁ –C ₂ str
ν_5	1468	31.9	10	1511	115.67	–25	ring def
ν_6	1457	12.4	28	1496	62.96	+24	ring def + C–H wag
ν_7	1416	19.7	22	1447	83.73	+3	C–H wag + ring def
ν_8	1345	0.5		1294	0.36	–8	C–H wag + ring def
ν_9	1236	34.5	12	1260	108.79	+4	ring def + C–F str
ν_{10}	1177	0.9		1156	21.06	–45	ring def
ν_{11}	1121	6.5	31	1136	7.67	–38	C–H wag
ν_{12}	1032	0.8		1040	13.30	+56	ring def
ν_{13}	919	20.3	22	928	76.62	+17	ring def + C–F str
ν_{14}	782	0.1		784	0.49	–78	ring def + C–F str
ν_{15}	540	8.8	20	555	30.88	+2	C–F str + ring def
ν_{16}	484	9.3	7	459	39.87	+12	ring def + C–F wag
ν_{17}	411	0.1		404	17.12	+3	C–F wag + ring def
$\nu_{18} a''$	862	0.6	z	948	0.86	z	C–H oop wag
ν_{19}	847	<0.1	z	876	4.33	z	C–H oop wag
ν_{20}	749	38.4	z	752	64.06	z	C–H oop wag
ν_{21}	565	0.3	z	614	0.40	z	ring oop def
ν_{22}	514	<0.1	z	559	<0.1	z	ring torsion
ν_{23}	457	0.6	z	441	0.51	z	ring torsion
ν_{24}	220	0.4		224	0.24	z	ring oop def

^a ν = wavenumber in cm⁻¹, I = IR intensity in km/mol, ϕ = in-plane transition moment angle (Figure 6) in deg, and A = Raman scattering activity in Å⁴/amu. ^b See Figure 6 for the definition of ϕ . The estimated experimental error limits are $\pm 17^\circ$ for ϕ close to 0° and 90° , and $\pm 9^\circ$ for ϕ close to 45° . ^c Unscaled.

by the calculations (both in the order and magnitude—see Tables 1 and 2).

Initial ab initio calculations (HF/6-31G*) performed for **1a** predicted that the transition moment of the triple bond stretching vibration should be substantially inclined (33°) from the axis bisecting the 1–2 and 4–5 bonds. Moreover, a large intensity increase with respect to that of **1** was predicted (118 km/mol vs 0.05 km/mol). However, the experimentally determined intensity of the triple bond stretching band was found to be still quite low (3.9 km/mol). The MP2/6-311G** calculation yielded a value of 2.4 km/mol, evidently in much better agreement with experiment. Interestingly, the present DFT B3LYP/cc-pVDZ predictions, which are otherwise superior to those obtained with the MP2 method, substantially overestimate the intensity of this transition, yielding a value of 45.3 km/mol.

The results obtained with the DFT approach gave slightly better overall agreement with experiment and are therefore presented in more detail; the calculated fundamental vibrational wavenumbers, IR intensities, and Raman scattering activities for **1**, **1a**, and **1b** are listed in Tables 1–3. Regression of all 63 fundamental wavenumbers observed for the three *o*-benzyne on the corresponding calculated ones led to the least-squares scaling relation, $\nu^{\text{obsd}} = 0.9671\nu^{\text{calcd}}$, with a standard deviation of 39 cm⁻¹. In view of the general difficulties in the description

TABLE 2: Observed and Calculated Fundamental Vibrational Transitions for Perfluoro-*o*-benzyne (1b)^a

	exptl ^b		exptl ^c		B3LYP/cc-pVDZ			approximate description
	$\tilde{\nu}$	<i>I</i>	$\tilde{\nu}$	<i>I</i>	$\tilde{\nu}^d$	<i>I</i>	<i>A</i>	
ν_1 a ₁	1878.4	0.8	1878.6	0.5	2031	0.50	13.20	C ₁ –C ₂ str
ν_2	1497.6	19.1	1499.7	8.4	1511	22.70	15.49	C ₄ –C ₅ str + ring def
	1492.9	10.7						
ν_3	1456.9	13.2	1457.6	12.0	1486	159.62	5.28	ring breath + C–F str
			1459.1	15.1				
ν_4			1349.1	0.7	1298	3.94	10.82	ring def
ν_5	1076.4	20.5	1076.5	81.0	1094	131.07	1.51	C–F str + ring def
	1074.0	14.2						
ν_6	699.1	8.5	699.3	8.9	706	10.04	24.17	ring str
ν_7	442.8	0.3			451	0.04	5.54	ring bend
ν_8	312.2	2.9			315	0.95	0.11	C–F wag
ν_9	271.0	0.5			274	0.01	0.13	C–F wag
ν_{10} a ₂					696	0	0.34	ring torsion
ν_{11}					430	0	3.94	ring oop def + C–F wag
ν_{12}					381	0	0.72	C ₁ –C ₂ torsion
ν_{13}					156	0	0.05	C–F wag
ν_{14} b ₁	577.8	0.6			628	1.30	0.03	ring oop def + C–F wag
ν_{15}	331.4	4.7			343	1.16	1.63	ring oop def + C–F wag
ν_{16}	140.0	<0.1			142	0.56	0.62	ring oop def + C–F wag
ν_{17} b ₂	1558.8	16.7	1555.8	13.2	1573	15.73	1.97	ring def
ν_{18}	1486.5	164.0	1486.5	217.0	1528	562.64	0.84	C–F str + ring def
ν_{19}	1214.0	27.5	1217.0	30.2	1230	21.54	2.79	C–F str + ring def
ν_{20}	980.2	31.2	974.0	149.0	986	255.67	0.06	C–F str + ring def
	971.4	37.2						
ν_{21}	642.0	0.2	657.0	<0.1	658	<0.01	0.55	C–F wag
ν_{22}	586.0	13.6	586.2	14.1	551	19.57	1.34	ring bend
ν_{23}	463.6	12.1	465.1	10.2	448	38.00	16.70	ring bend
ν_{24}	296.4	0.7			277	2.79	0.01	C–F wag

^a $\tilde{\nu}$ = wavenumber in cm^{−1}, *I* = IR intensity in km/mol, and *A* = Raman scattering activity in Å⁴/amu. ^b Relaxed form (see text). ^c Compressed form (see text). ^d Unscaled.

TABLE 3: Observed and Calculated Fundamental Vibrational Transitions for *o*-benzyne (1)^a

	exptl ^b		B3LYP/cc-pVDZ			approximate description
	$\tilde{\nu}$	<i>I</i>	$\tilde{\nu}^c$	<i>I</i>	<i>A</i>	
ν_1 a ₁	3094	5.7	3207	5.50	373.82	C–H str
ν_2	3071	0.9	3182	4.59	140.29	C–H str
ν_3	1846	2.0	2022	0.02	15.20	C ₁ –C ₂ str
ν_4	1415	0.1	1484	0.75	10.18	ring str + C–H wag
ν_5	1271	1.3	1315	0.66	18.62	ring str + C–H wag
ν_6	1055	7.4	1153	0.05	2.70	ring str + C–H wag
ν_7	1039	10.4	1081	22.59	25.32	ring str
ν_8	982	5.2	1000	7.31	15.55	ring str + C–H wag
ν_9	582	0.1	620	0.43	4.04	ring bend
ν_{10} a ₂			973	0	0.08	C–H oop wag
ν_{11}			870	0	3.55	C–H oop wag
ν_{12}			598	0	0.19	ring torsion
ν_{13}			437	0	0.63	ring torsion
ν_{14} b ₁	838	0.3	921	0.01	1.08	C–H oop wag
ν_{15}	737	47.4	751	58.28	2.97	C–H oop wag
ν_{16}	388	4.2	393	4.20	0.11	ring oop def
ν_{17} b ₂	3086	9.1	3203	29.40	4.68	C–H str
ν_{18}	3049	0.6	3166	0.98	85.41	C–H str
ν_{19}	1451	9.1	1472	11.56	7.29	ring str + C–H wag
ν_{20}	1394	5.5	1423	4.81	0.10	ring str + C–H wag
ν_{21}	1307	0.2	1260	0.11	3.66	C–H wag
ν_{22}	1094	1.3	1103	1.49	10.83	C–H wag
ν_{23}	849	24.8	839	30.25	0.50	ring bend
ν_{24}	472	81.0	404	112.84	17.74	ring bend

^a $\tilde{\nu}$ = wavenumber in cm^{−1}, *I* = IR intensity in km/mol, and *A* = Raman scattering activity in Å⁴/amu. ^b Reference 6. ^c Unscaled.

of the electronic structure of benzyne, this result may be considered as very satisfactory.

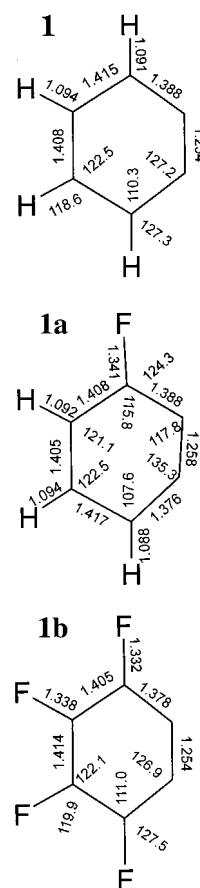


Figure 3. B3LYP/cc-pVDZ equilibrium geometries for *o*-benzyne (**1**), perfluoro-*o*-benzyne (**1b**), and 3-fluoro-*o*-benzyne (**1a**). Bond lengths are given in Å, and bond angles are given in deg.

The MP2 calculations yielded better values for the triple bond stretching vibration, regarding wavenumber and intensity. On the other hand, the predicted frequency shift upon going from **1a** to **1b** is incorrect for MP2, whereas the DFT results agree with experiment.

Site Decompression and High-Resolution Spectra. We have been able to obtain highly resolved spectra of the fluorinated benzyne (**1a** and **1b**) by using a technique that we call “site decompression”. This method utilizes the static pressure created during photochemical transformations and relaxation effects (pressure release) occurring during warm-up of solid matrices. In the rigid environment, the anhydride molecules are tightly surrounded by matrix atoms. Photochemical fragmentation replaces a single anhydride molecule with three molecules: benzyne, CO, and CO₂. For the reaction proceeding in the gas phase, the volume of the products would be slightly larger than the volume of the precursor. However, in our case, the reaction proceeds in a highly incompressible environment and results in a hydrostatic pressure exerted by the products on each other as well as on the surroundings. This leads to shifts of the absorption frequencies for all fragments. Previous studies of mechanical stress caused by reactions in molecular crystals have demonstrated that the shifts of the ν_3 asymmetric stretching vibration of CO₂ can be used to estimate the magnitude of the pressure in the cavity.^{47–50} A shift to the blue (higher frequency) of 0.4 cm^{−1} corresponds to 1 kbar of increase of the pressure.⁵⁰ However, in the absence of calibration studies, it is not obvious to what extent these results are transferable to pressure determination in matrices.

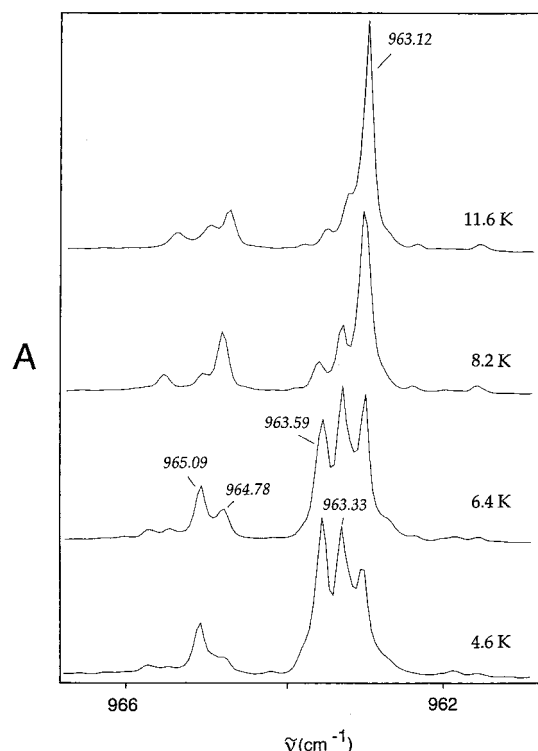


Figure 4. The spectral changes in a “site cluster” in an Ar matrix containing (**1b**) during gradual warm-up from 4.6 to 11.6 K. The top trace corresponds to fully relaxed matrix, while bottom curve originates from the mixture of compressed and relaxed molecules after initial irradiation at 308 nm.

An example of this phenomenon in matrices is presented in Figure 2, which was produced by taking advantage of the high static pressure created by photochemical fragmentation in the solid noble-gas matrix cavity (kept at about 4.6 K) initially filled with the anhydride **2b**. The increase in the total volume of the photofragments with respect to that of the precursor in this highly incompressible environment results in a high static pressure exerted on C_6F_4 by CO and CO_2 . However, gentle warm-up of the matrix (by less than 10 K) allows the molecules to reorient slightly, and pressure is thus released. We measured spectra of both the initial “compressed” sample and of the “relaxed” sample (Figure 4). The difference between these two exhibits very narrow lines (Figure 2), with individual line widths of less than 0.1 cm^{-1} (limited by instrument resolution). The advantage of this technique lies in the fact that it virtually removes the unwanted background absorptions originating from the unreacted anhydride **2** and minor impurities. A prerequisite for a successful application of this method is that the relaxation produces changes in population between discrete levels rather than gradual spectral shifts. This is indeed observed, similarly to what has been reported previously for molecular crystals.⁴⁷

The merits of the “site decompression” technique become obvious when compared with the usually available and employed procedures for obtaining difference spectra. Using a standard approach of subtracting the initial spectra from those obtained after irradiation often leads to spectral artifacts. Under any of the examined irradiation conditions (various wavelengths), two phenomena always happen in our experiments and complicate the extraction of the sought-after spectral details. First, the yields of the photolysis of the anhydride **2** differ significantly for various matrix sites. For some minor sites, the difference amounts to a factor of 5, and thus simple subtraction of the precursor from the partially photoconverted sample

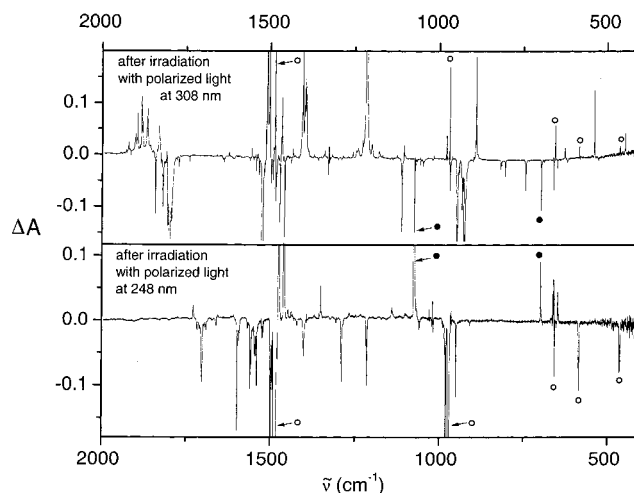


Figure 5. Linear dichroism spectrum of perfluoro-*o*-benzynes (**1b**) photooriented by 308 nm (top trace) and by 248 nm irradiation (bottom trace) and of the remaining perfluorophthalic anhydride isolated in an Ar matrix at 12 K. Solid dots indicate a_1 vibrations; open circles indicate b_2 vibrations.

produces derivative-like spectra. This makes the spectral assignments somewhat arbitrary and incomplete, especially for the weakest bands in the regions where there is an overlap between the product and precursor absorptions. Second, the quantitative conversion of the initial anhydride sample exclusively to C_6F_4 , CO, and CO_2 does not seem to be possible under any photochemical conditions that we have examined. At the “best” wavelengths, 308, 248, or 254 nm, facile conversion of the anhydride is always accompanied by much slower (by at least an order of magnitude) secondary photochemical reactions. Upon absorption of the next-arriving photons, some of the earlier created C_6F_4 molecules slowly photoreact with CO and CO_2 , because we observe the decrease of their intensities. Some C_6F_4 presumably decomposes to difluoroacetylene, as witnessed by a weak absorption at 1341 cm^{-1} , which has been previously ascribed to this species.⁵¹ Under any circumstances, the “clean” spectra of the benzynes can be produced only by some kind of “approximate” spectral manipulation. We find that the “site decompression” procedure described above leads to the “cleanest” and the best-resolved spectra of C_6F_4 , and it is much more efficient in data deconvolution than a simple removal of the precursor spectrum. In Figure 2, we present only the positive half of the difference spectrum, corresponding to the less-perturbed, “relaxed” C_6F_4 . Although, the term “high resolution” is relative, because the majority of the IR absorption spectra of reactive intermediates in matrices is reported in the literature with resolution of $0.5\text{--}1\text{ cm}^{-1}$, we believe that it is appropriate to the case presented here.

Polarization Results. Figure 5 presents IR linear dichroism (LD) spectra for **1b**, obtained after photolysis of the phthalic anhydride precursor with linearly polarized 308 or 248 nm light. In a rigid environment, both the remaining precursor and the ensuing photoproduct become partially oriented. The LD curves represent the difference in the absorption of light polarized parallel and perpendicular to the electric vector of the photolyzing radiation. The sign of the resulting IR LD signal is determined by the electronic transition moment direction in the precursor and by the symmetry species of a particular vibration. It has been observed⁶ that irradiation of **2** with polarized 248 nm light leads to a negative IR LD sign for a_1 and b_1 vibrations and to a positive sign for b_2 species in the photoproduct *o*-benzynes. Using 308 nm excitation produces negative LD for

TABLE 4: Vibrational Frequencies Determined for Molecules Engaged in the Phototransformation Leading from Phthalic Anhydride to Benzyne (See Scheme 1)

compound	IR ^a	UV ^b
perfluorophthalic anhydride (2b)	1843 (s), 1802 (vs), 1524 (s), 1511 (vs), 1408 (m), 1329 (m), 1220 (s), 1114 (m), 948 (s), 929 (s), 893 (m), 807 (w), 736 (w)	304 (sh), 301 (st), 248 (br), 212 (br)
perfluorocyclopentadienyldieneketene (3b)	2089 (vs)	288 (st)
perfluorobenzocyclopropenone (6b)	1908 (s), 1860 (s), 1496 (vs), 1470 (vs), 1289 (m), 1109 (s), 1052 (s), 949 (s), 929 (s), 821 (m), 652 (m), 623 (m)	271 (st), 238 (br)
3-fluorophthalic anhydride (2a)	1874 (s), 1799 (vs), 1619 (m), 1489 (s), 1352 (m), 1282 (w), 1271 (m), 1264 (s), 1257 (m), 1216 (s), 1132 (s), 961 (w), 825 (w), 781 (w), 740 (s)	301 (st), 240 (br), 220 (st), 197 (br)
3-fluorocyclopentadienyldieneketene (3a)	2080 (vs)	283 (st)
3-fluorobenzocyclopropenone (6a)	1848 (vs)	268 (st), 231 (br)

^a IR data in cm⁻¹; relative intensities: s-strong, vs-very strong, m-medium, w-weak. ^b UV-vis data in nm; sh-shoulder, st-structured, br-broad.

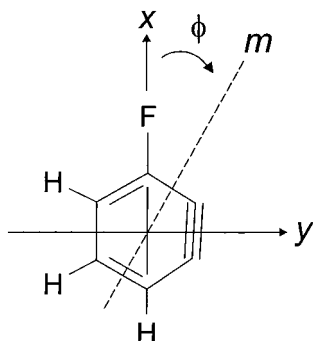


Figure 6. Definition of in-plane transition moment angles, ϕ , for 3-fluoro-*o*-benzyne (**1a**). Positive ϕ is measured from x to y , where x is the axis passing through carbon centers C6 and C3, and y is defined as indicated (y can be considered to be almost parallel to a line passing through the midpoints of the C4–C5 and C1–C2 bonds).

b_1 and b_2 vibrations and a positive sign for a_1 species. These two experimental situations are illustrated in Figure 5. Thus, the analysis of the IR LD signs obtained after irradiation with polarized light at two wavelengths corresponding to different transition moment directions in the precursor makes it possible to make absolute polarization assignments.

While the determination of transition moment directions is straightforward for high-symmetry molecules, such as **1b**, certain assumptions have to be made in the case of lower-symmetry compounds.⁵² We use the following labeling of molecular axes for **1a** (Figure 6): z = out-of-plane, x = passing through the centers C3 and C6, practically parallel to the C–F bond, and y = in-plane, perpendicular to x and z . In the laboratory coordinate system, light propagates along the direction X and is linearly polarized along the Z axis. Using at first unpolarized ultraviolet light (308 nm, excimer laser), we convert most of the precursor to **1a**. Only then is the sample exposed to polarized light at 248 nm. Partial destruction of **1a** produces a sample uniaxially oriented about the Z axis. Polarization measurements indicate that the UV transition moment is polarized approximately along the C–F bond, that is, essentially along the x axis, because a negative dichroism is observed in the IR for the C–F stretch. All vibrations for which the IR dichroism could be determined fall into two distinct classes, depending on the value of the observed dichroic ratio. The same dichroic ratio should be observed for all out-of-plane vibrations. This is not the case for in-plane vibrations, which may be polarized along any direction in the plane, and the dichroic ratio may thus be different for each transition. We have identified five out-of-plane infrared transitions in **1a**. For each experiment, and thus for a given degree of photoconversion, all of these transitions had (within experimental error) the same dichroic ratio, $d_z = E_z/E_y$. By use of the value of this ratio, the value of the

orientation factor, $K_z = d_z/(1 + 2d_z)$, can be determined.⁵³ The other two principal orientation factors can then be determined from the definition of the uniaxial orientation, $K_y = K_z = (1 - K_x)/2$. For transitions i , polarized in the molecular plane, we then have

$$\tan^2 \phi_i = (K_y - K_i)/(K_i - K_x)$$

where ϕ_i is the angle between the transition moment, m_i , for the i -th transition and the molecular axis x (Figure 6).

Using this formula for **1a**, we have obtained the in-plane transition moment angles, $|\phi|$, compiled in Table 1. The angles listed in this table were obtained by averaging results from several independent measurements. The errors are on average about $\pm 17^\circ$ for angles close to 0° and 90° and $\pm 9^\circ$ for those close to 45° . This procedure does not allow for a determination of the sign of ϕ .

The variation of the observed moment angles (Table 1) obviously reflects the low molecular symmetry of **1a** (C_s). The perturbation of the *o*-benzyne skeleton is large enough to activate the otherwise inactive infrared modes (a_2 in the C_{2v} structure) and to incline the in-plane transition moments away from the C_{2v} symmetry axes. In view of the results of the “calibration” studies⁵⁴ of the quality of theoretical transition moment determination, the agreement between experimentally determined and predicted transition moment directions is very good, given the relatively modest level of theoretical approximation applied at present. It should be stressed, however, that the *o*-benzyne represent a difficult case for theory,⁵⁵ as witnessed by problems with intensity and frequency shifts of the CC triple bond stretching vibration upon fluorine substitution.

Side Products and Their Electronic and IR Absorption Spectra. The phototransformation of the phthalic anhydride into benzyne is accompanied by the formation of benzocyclopropenone (**6**), as well as other products of photolytic and thermal reactions: cyclopentadienyldieneketene (**3**), hex-1-ene-3,5-diyne (**5**), and biphenylenes (**4**) (Scheme 1). We have obtained the detailed electronic and IR absorption spectra for these molecules. The spectra were interpreted and structures were assigned on the basis of very good agreement between experimental data and theoretical predictions for these and related hydrogenated compounds. The side-products identification is based on the comparison of the observed IR absorptions and calculated vibrational spectra for structures **3** and **6**. The positions of the observed characteristic absorptions in these compounds are highly compatible with well-established absorptions of the cumulative double bond in parent **3**⁵⁶ and carbonyl stretch in parent **6**.⁶ Simultaneous determination of the IR and UV-vis absorption spectra allows for subsequent assignment of the electronic features. The compounds **4a** and **4b** were identified

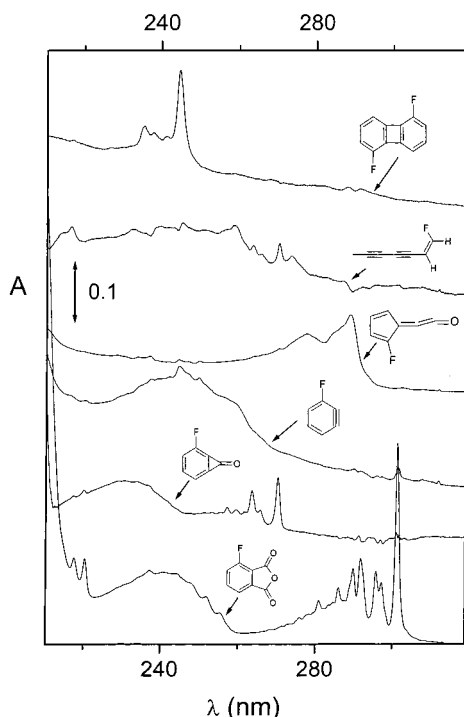


Figure 7. Electronic absorption spectra of (from bottom to top) 3-fluorophthalic anhydride (**2a**), 3-fluorobenzocyclopropanone (**6a**), 3-fluoro-*o*-benzynes (**1a**), 2-fluorocyclopentadienylideneketene (**3a**), fluorohept-1-ene-3,5-diyne (**5a**), and a mixture of *cis*- and *trans*-3,9-difluorobiphenylenes (**4a**).

with the help of GC–MS, in which molecular ions of the dimers were present. In case of **4a**, no *cis* or *trans* conformers were separated or identified, but the absorption of the warm-up product of **1b** was assigned to **4b** by comparison with absorption of authentic sample obtained from irradiation of **2b** in solution. The prominent IR frequencies and the UV absorption features are presented in Table 4, while the electronic spectra are shown in Figure 7.

4. Summary and Conclusions

We have prepared and identified two fluoro-substituted benzynes, 3-fluoro-*o*-benzynes (**1a**) and perfluoro-*o*-benzynes (**1b**). This represents the first direct observation of **1a**, for which a complete set of 24 IR vibrational fundamental wavenumbers is reported and assigned, including the triple bond stretching vibration at 1866 cm^{-1} . Compound **1b** was recently investigated by Wenk and Sander.³⁸ We extend the results of this investigation by observing kinetics of dimerization for **1b** and by providing an almost complete set of fundamental wavenumbers; most of these are previously unreported, such as the weak triple bond stretching at 1878 cm^{-1} . The assignments of the vibrational transitions were supported by the application of polarization spectroscopic techniques, which provide information on transition moment directions, and by the results of DFT quantum chemical calculations. The results confirm a previous assignment of the triple bond stretching vibration in parent *o*-benzynes (**1**)⁶ and extend the data basis for further refinement of theoretical methods. In addition, vibrational and electronic spectra were obtained for several transient intermediates involved in the fluorobenzynes photogeneration, as well as for the final products of benzyne dimerization.

By taking advantage of the pressure relaxation occurring in a solid matrix upon gentle warming, it was possible to remove signals due to unreacted precursor, side products, and impurities

and to obtain highly resolved IR spectra of the target fluorobenzynes with high sensitivity. Application of this technique enabled the observation of weak transitions that would otherwise easily escape detection (like the triple bond stretching band of **1b**³⁸). We recommend this technique as having great potential for solid-phase spectral studies of reactions that are accompanied by volume changes.

Acknowledgment. This research was supported by the internal NREL funds (“FIRST” program). We would like to thank Prof. Rudolf Zahradník for stimulating discussions.

References and Notes

- (1) Wentrup, C. *Reactive Molecules*; John Wiley and Sons: New York, 1984; p 288.
- (2) *Organic Reactive Intermediates*; McManus, S. P., Ed.; Academic Press: New York, 1973; p 449.
- (3) Moody, C. J.; Whitham, G. H. *Reactive Intermediates*; Oxford University Press: Oxford, U.K., 1992; p 68.
- (4) Hoffman, R. W. *Dehydrobenzene and Cycloalkynes*; Academic Press: New York, 1967.
- (5) Gilchrist, T. L.; Arynes. In *The Chemistry of triple-bonded functional groups*; Patai, S.; Rappoport, Z., Eds.; The Chemistry of Functional Groups, Supplement C; Wiley: Chichester, U.K., 1983; pp 383–419.
- (6) Radziszewski, J. G.; Hess, B. A., Jr.; Zahradník, R. *J. Am. Chem. Soc.* **1992**, *114*, 52 and references therein.
- (7) Diau, E. W.-G.; Casanova, J.; Roberts, J. D.; Zewail, A. H. *Proc. Natl. Acad. Sci. U.S.A.* **2000**, *97*, 1376.
- (8) Warmuth, R. *Angew. Chem., Int. Ed. Engl.* **1997**, *36*, 1347.
- (9) Wentrup, C.; Blanch, R.; Briehl, H.; Gross, G. *J. Am. Chem. Soc.* **1988**, *110*, 1874.
- (10) Armstrong, R. J.; Brown, R. F. C.; Eastwood, F. W.; Romyn, M. *E. Aust. J. Chem.* **1979**, *32*, 1767.
- (11) Barry, M.; Brown, R. F. C.; Eastwood, F. W.; Gunawardana, D. A.; Vogel, C. *Aust. J. Chem.* **1984**, *37*, 1643.
- (12) Brown, R. F. C.; Browne, N. R.; Coulston, K. J.; Danen, L. B.; Eastwood, F. W.; Irvine, M. J.; Pullin, D. E. *Tetrahedron Lett.* **1986**, *27*, 1075.
- (13) Brown, R. F. C.; Browne, N. R.; Coulston, K. J.; Eastwood, F. W.; Irvine, M. J.; Pullin, D. E.; Wiersum, U. E. *Aust. J. Chem.* **1989**, *42*, 1321.
- (14) Schweig, A.; Münzel, N.; Meyer, H.; Heidenreich, A. *Struct. Chem.* **1989**, *1*, 89.
- (15) Simon, J. G. G.; Münzel, N.; Schweig, A. *Chem. Phys. Lett.* **1990**, *170*, 187.
- (16) Münzel, N.; Schweig, A. *Chem. Phys. Lett.* **1988**, *147*, 192.
- (17) Orendt, A. M.; Facelli, J. C.; Radziszewski, J. G.; Horton, W. J.; Grant, D. M.; Michl, J. *J. Am. Chem. Soc.* **1996**, *118*, 846.
- (18) Scheiner, A. C.; Schaefer, H. F., III *J. Am. Chem. Soc.* **1992**, *114*, 4758.
- (19) Scheiner, A. C.; Schaefer, H. F., III; Liu, B. *J. Am. Chem. Soc.* **1989**, *111*, 3118.
- (20) Burton, N. A.; Quelch, G. E.; Gallo, M. M.; Schaefer, H. F., III *J. Am. Chem. Soc.* **1991**, *113*, 764.
- (21) Rigby, K.; Hillier, I. H.; Vincent, M. *J. Chem. Soc., Perkin Trans. 2* **1987**, *2*, 117.
- (22) Radom, L.; Nobes, R. H.; Underwood, D. J.; Li, W. K. *Pure Appl. Chem.* **1986**, *58*, 75.
- (23) Leopold, D. G.; Miller, A. E. S.; Lineberger, W. C. *J. Am. Chem. Soc.* **1986**, *108*, 1379.
- (24) Nam, H. H.; Leroi, G. E. *Spectrochim. Acta, Part A* **1985**, *41*, 67.
- (25) Dewar, M. J. S.; Ford, G. P.; Rzepa, H. S. *J. Mol. Struct.* **1979**, *51*, 275.
- (26) Farnell, L.; Radom, L. *Chem. Phys. Lett.* **1982**, *91*, 373.
- (27) Taylor, P. R. *J. Comput. Chem.* **1984**, *5*, 589.
- (28) Brown, R. D.; Ditman, R. G. *Chem. Phys. Lett.* **1984**, *83*, 77.
- (29) Langenaeker, W.; De Proft, F.; Geerlings, P. *J. Phys. Chem. A* **1998**, *102*, 5944.
- (30) Pittman, C. U., Jr.; Saebo, S.; Xu, H. *J. Org. Chem.* **2000**, *65*, 6620.
- (31) Lindh, R.; Bernhardsson, A.; Schütz, M. *J. Phys. Chem. A* **1999**, *103*, 9913.
- (32) Cramer, C. J.; Nash, J. J.; Squires, R. R. *Chem. Phys. Lett.* **1997**, *277*, 311.
- (33) Johnson, W. T. G.; Cramer, C. J. *J. Am. Chem. Soc.* **2001**, *123*, 923.
- (34) Deng, W.-Q.; Han, K.-L.; Zhan, J.-P.; He, G.-Z. *Chem. Phys. Lett.* **1998**, *288*, 33.
- (35) De Visser, S. P.; Filatov, M.; Shaik, S. *Phys. Chem. Chem. Phys.* **2000**, *2*, 5046.

- (36) Jiao, H.; von Ragué Schleyer, P.; Beno, B. R.; Houk, K. N.; Warmuth, R. *Angew. Chem., Int. Ed. Engl.* **1997**, *36*, 2761.
- (37) Liu, R.; Zhou, X.; Pulay, P. *J. Phys. Chem.* **1992**, *96*, 8336.
- (38) Wenk, H. H.; Sander, W. *Chem.—Eur. J.* **2001**, *7*, 1837.
- (39) Heaney, H. *Fortschr. Chem. Forsch.* **1970**, *16*, 35.
- (40) Callander, D. D.; Coe, P. L.; Tatlow, J. C. *Chem. Commun.* **1966**, 143; *Tetrahedron*, **1969**, *25*, 25.
- (41) Brewer, J. N. P.; Eckhard, I. F.; Heaney, H.; Marples, B. A. *J. Chem. Soc. C* **1968**, 664.
- (42) Yamamoto, G.; Suzuki, M.; Oki, M. *Bull. Chem. Soc. Jpn.* **1983**, *56*, 809.
- (43) Hayashi, S.; Ishikawa, N. *Bull. Chem. Soc. Jpn.* **1972**, *45*, 642.
- (44) Gribble, G. W.; Kelly, W. J. *Tetrahedron Lett.* **1981**, *22*, 2475.
- (45) Lu, C. In *Methods and Phenomena. Their Application in Science and Technology*; Volsky, S. P., Czanderna, A. W., Eds.; Elsevier: Amsterdam, 1984; Vol. 7, p 19.
- (46) Frisch, M. J.; Trucks, G. W.; Schlegel, H. B.; Scuseria, G. E.; Robb, M. A.; Cheeseman, J. R.; Zakrzewski, V. G.; Montgomery, J. A., Jr.; Stratmann, R. E.; Burant, J. C.; Dapprich, S.; Millam, J. M.; Daniels, A. D.; Kudin, K. N.; Strain, M. C.; Farkas, O.; Tomasi, J.; Barone, V.; Cossi, M.; Cammi, R.; Mennucci, B.; Pomelli, C.; Adamo, C.; Clifford, S.; Ochterski, J.; Petersson, G. A.; Ayala, P. Y.; Cui, Q.; Morokuma, K.; Malick, D. K.; Rabuck, A. D.; Raghavachari, K.; Foresman, J. B.; Cioslowski, J.; Ortiz, J. V.; Stefanov, B. B.; Liu, G.; Liashenko, A.; Piskorz, P.; Komaromi, I.; Gomperts, R.; Martin, R. L.; Fox, D. J.; Keith, T.; Al-Laham, M. A.; Peng, C. Y.; Nanayakkara, A.; Gonzalez, C.; Challacombe, M.; Gill, P. M. W.; Johnson, B. G.; Chen, W.; Wong, M. W.; Andres, J. L.; Head-Gordon, M.; Replogle, E. S.; Pople, J. A. *Gaussian 98*, revision A.3; Gaussian, Inc.: Pittsburgh, PA, 1998.
- (47) McBride, J. M.; Segmuller, B. E.; Hollingsworth, M. D.; Mills, D. E.; Weber, B. A. *Science*, **1986**, *234*, 830.
- (48) McBride, J. M.; Hollingsworth, M. D. *Mol. Cryst. Liq. Cryst.* **1988**, *161*, 25.
- (49) McBride, J. M.; Hollingsworth, M. D. *Adv. Photochem.* **1990**, *15*, 279.
- (50) Hanson, R. C.; Jones, L. H. *J. Chem. Phys.* **1981**, *75*, 1102.
- (51) Brahms, J. C.; Daily, W. P. *J. Am. Chem. Soc.* **1989**, *111*, 3071.
- (52) Raabe, G.; Vancik, H.; West, R.; Michl, J. *J. Am. Chem. Soc.* **1986**, *108*, 671.
- (53) Michl, J.; Thulstrup, E. W. *Spectroscopy with Polarized Light. Solute Alignment by Photoselection, in Liquid Crystals, Polymers, and Membranes*; VCH Publishers Inc.: New York, 1986.
- (54) Radziszewski, J. G.; Downing, J.; Gudipati, M. S.; Balaji, V.; Thulstrup, E. W.; Michl, J. *J. Am. Chem. Soc.* **1996**, *118*, 10275.
- (55) Hess, B. A., Jr.; Schaad, L. J. *Mol. Phys.* **2000**, *98*, 1107.
- (56) Radziszewski, J. G.; Kaszynski, P.; Friderichsen, A.; Abildgaard, J. *Collect. Czech. Chem. Commun.* **1998**, *63*, 1094.